COMPRESSSIVE AND BENDING BEHAVIOR OF STRIP-SHAPED FIBER-REINFORCED ELASTOMERIC BEARINGS

S. Pinarbasi[1], Y. Mengi[2] and U. Akyuz[3]

[1] *Research Assistant, Dept. of Civil Engineering, Kocaeli University, Kocaeli, Turkey*
[2] *Professor, Dept. of Engineering Sciences, Middle East Technical University, Ankara, Turkey*
[3] *Assoc. Professor, Dept. of Civil Engineering, Middle East Technical University, Ankara, Turkey*
Email: seval.pinarbasi@kou.edu.tr, meng@metu.edu.tr, han@metu.edu.tr

ABSTRACT :

Multi-layered steel-reinforced elastomeric bearings have widely been used for isolation of structures and machines from vibrations. In an attempt to develop light-weight and low-cost isolators, recent studies have proposed the use of fiber reinforcement in place of steel reinforcement. Although the "rigid" reinforcement assumption is a fairly reasonable assumption in the analysis of a steel-reinforced bearing, it is necessary to include the effect of reinforcement flexibility while studying the compressive or bending behavior of a fiber-reinforced bearing. The main objective of this paper is to study, in detail, the compressive and bending behavior of fiber-reinforced elastomeric bearings by using advanced analytical solutions recently derived by Pinarbasi and Mengi (2008). Free from two of the three fundamental assumptions commonly used in the "pressure" method, these closed-form solutions are valuable tools for a detailed study on behavior of fiber-reinforced bearings under uniform compression or/and pure bending. Analyses conducted on bearings with different geometrical and material properties show that the compressive/bending behavior of a fiber-reinforced bearing can be considerably different than that of its steel-reinforced counterpart. The effect of reinforcement flexibility is very similar to the effect of material compressibility. As expected, the effect of reinforcement flexibility highly depends on the geometrical and material properties of the bearing. Reinforcement flexibility is found to be most effective when the "shape" factor of the bearing is large and Poisson's ratio of the layer material is close to 0.5.

KEYWORDS: Seismic isolation, fiber-reinforced elastomeric bearing, rubber, compression, bending, flexible reinforcement

1. INTRODUCTION

Multi-layered steel-reinforced elastomeric bearings have widely been used for isolation of machines, bridges and recently of structures from vibrations like earthquake excitations. In an attempt to develop light-weight, low-cost isolators to be used in developing countries and/or low-cost housing, recent studies (e.g., Kelly, 2002; Moon et al., 2002; Tsai, 2004) have proposed the replacement of steel reinforcement with fiber reinforcement.

Although the "rigid" reinforcement assumption can realistically be used in the analysis of a steel-reinforced bearing, it is necessary to include the effect of reinforcement flexibility while investigating the compressive or bending behavior of a fiber-reinforced bearing. Recently, compressive/bending behavior of strip-shaped elastic layers bonded to flexible reinforcements has been analyzed using an approximate theory based on modified Galerkin method (Pinarbasi and Mengi, 2008). Since the approximate theory eliminates two of the three fundamental assumptions of the commonly-used pressure method, i.e., the "pressure" and the plane sections remain plane assumptions (refer to Kelly (1997) for details on the pressure method), the solutions derived using this theory are advanced in view of that they are valid not only for a strictly or nearly incompressible bearing with high shape factor (HSF), but even for a compressible bearing with low shape factor (LSF). It is to be noted that only remaining assumption in the derived expressions is the parabolic bulging assumption. This assumption has already been shown to be realistic unless the thickness of the individual elastomer layers in the bearing is

enormously large. Accordingly, these advanced solutions can be used as valuable tools for a detailed study on compressive/bending behavior of fiber-reinforced elastomeric bearings.

The main objective of this paper is to study compressive and bending behavior of strip-shaped fiber-reinforced elastomeric bearings using the analytical solutions derived from the above-mentioned higher order theory. Main emphasis is given to the investigation of the influence of reinforcement flexibility on effective bearing moduli, i.e., effective compression and bending moduli, and on stress distributions in the bearing. Since the effect of reinforcement flexibility also depends on the geometrical and material properties of the bearing itself, the discussions inherently include a study on the effects of the other two basic parameters governing the bearing behavior; "shape factor" (ratio of one loaded area to bulge free areas for an interior rubber layer) of the bearing (S) and Poisson's ratio of the elastomeric material (ν).

2. CLOSED-FORM EXPRESSIONS FOR COMPRESSIVE AND BENDING BEHAVIOR OF FIBER-REINFORCED ELASTOMERIC BEARINGS

It is well known that the compressive or bending behavior of a multi-layered elastomeric bearing is governed by the behavior of its individual elastomer layers. Figure 1a shows the undeformed configuration for such an elastomer layer in a multi-layered fiber-reinforced strip. The layer has uniform thickness t and is bonded to flexible reinforcing sheets with equivalent thickness t_f at its top and bottom faces. Since the length of the layer is much larger than its width $2w$ and thickness t, the layer is in a state of plane strain and can be defined referring to a two-dimensional rectangular coordinate system (x_1, x_2) with its origin located at the center of the layer as shown in Figure 1a. When the layer is uniformly compressed, it deforms as shown in Figure 1b. On the other hand, under pure bending, the deformed shape takes the form shown in Figure 1c.

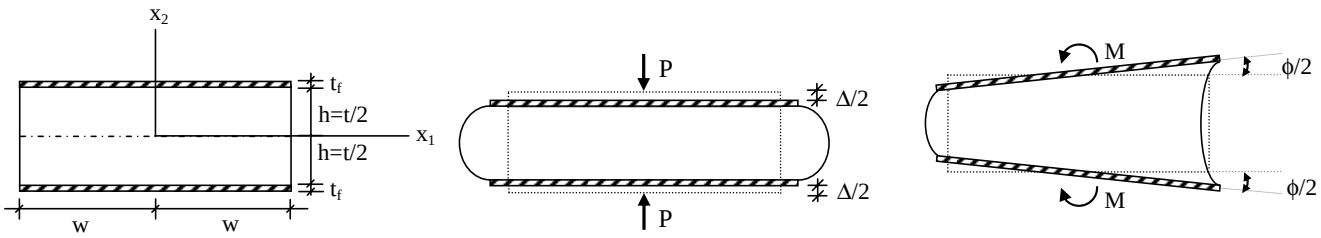

a. undeformed shape b. deformed shape under compression c. deformed shape under bending

Figure 1 Undeformed and deformed configurations for a fiber-reinforced elastomeric layer under uniform compression and pure bending

These compression and bending problems have recently been solved by Pinarbasi and Mengi (2008) using a higher order theory based on a modified version of Galerkin method (Mengi, 1980) and advanced closed-form solutions have been derived for displacement/stress distributions and effective layer moduli, i.e., compression and bending moduli. The following expressions for effective compression modulus E_c, effective bending modulus E_b and for displacement components u_1 and u_2 are directly taken from Pinarbasi and Mengi (2008):

- Uniform compression:

$$E_c = \alpha - \frac{\lambda^2}{\alpha}\frac{\beta_{10}^2}{\beta_1^2}\frac{\tanh(\beta_1 w)}{(\beta_1 w)} - \frac{\lambda^2}{\alpha}\frac{\beta_{11}^2}{\beta_1^2} \tag{2.1}$$

$$u_1 = \frac{3}{2}\frac{\Delta}{t}\frac{\lambda}{\alpha}\frac{\sinh(\beta_1 x_1)}{\beta_1\cosh(\beta_1 w)}\left(1-\frac{4x_2^{\,2}}{t^2}\right) + \frac{\Delta}{t}\frac{\lambda}{\alpha}\frac{\beta_{11}^2}{\beta_1^2}\left(x_1 - \frac{\sinh(\beta_1 x_1)}{\beta_1\cosh(\beta_1 w)}\right) \tag{2.2}$$

$$u_2 = \frac{30}{t}\frac{\lambda}{\alpha}\frac{\Delta}{t}\frac{x_2}{t}\left(1-\frac{4x_2^2}{t^2}\right)\left\{\begin{array}{l}\dfrac{1}{\beta_1\beta_{21}}\dfrac{\tanh(\beta_1 w)}{\sinh(\beta_{21}w)}\left[1-\dfrac{\mu+\lambda}{\mu}\dfrac{\beta_1^2}{\beta_1^2-\beta_{21}^2}\right]\cosh(\beta_{21}x_1)\\ +\dfrac{\mu+\lambda}{\mu}\dfrac{1}{\beta_1^2-\beta_{21}^2}\dfrac{\cosh(\beta_1 x_1)}{\cosh(\beta_1 w)}\end{array}\right\}-\frac{\Delta}{t}x_2 \tag{2.3}$$

- Pure bending:

$$E_b = \alpha-\frac{3\lambda^2}{\alpha}\frac{\beta_{10}^2}{\beta_1^2}\frac{1}{(\beta_1 w)^2}\left[\frac{(\beta_1 w)}{\tanh(\beta_1 w)}-1\right]-\frac{\lambda^2}{\alpha}\frac{\beta_{11}^2}{\beta_1^2} \tag{2.4}$$

$$u_1 = \left\{\begin{array}{l}\left[-\dfrac{3}{2}\dfrac{\lambda}{\alpha}\dfrac{\phi}{t}\dfrac{w\cosh(\beta_1 x_1)}{\beta_1\sinh(\beta_1 w)}+\dfrac{3}{2}\dfrac{\mu}{\alpha}\dfrac{\phi}{t}\dfrac{1}{\beta_{10}^2}\left(1+\dfrac{\beta_{10}^2}{\beta_1^2}\dfrac{\lambda}{\mu}\right)\right]\left(1-\dfrac{4x_2^2}{t^2}\right)\\ -\dfrac{\beta_{11}^2}{\beta_1^4}\dfrac{\lambda}{\alpha}\dfrac{\phi}{t}\dfrac{\beta_1 w}{\sinh(\beta_1 w)}\left[1-\cosh(\beta_1 x_1)\right]-\dfrac{\beta_{11}^2}{\beta_1^2}\dfrac{\lambda}{\alpha}\dfrac{\phi}{t}\dfrac{x_1^2}{2}\end{array}\right\} \tag{2.5}$$

$$u_2 = \frac{x_2}{t}\left(1-\frac{4x_2^2}{t^2}\right)\left(\begin{array}{l}-\dfrac{30}{t}\dfrac{\lambda}{\alpha}\dfrac{\phi}{t}\dfrac{w}{\beta_1\beta_{21}}\dfrac{\coth(\beta_1 w)}{\cosh(\beta_{21}w)}\left[1-\dfrac{\mu+\lambda}{\mu}\dfrac{\beta_1^2}{\beta_1^2-\beta_{21}^2}\right]\sinh(\beta_{21}x_1)\\ +\dfrac{5\phi}{2}\dfrac{\lambda}{\mu}\dfrac{\beta_{10}^2}{\beta_1^2}\dfrac{\sinh(\beta_{21}x_1)}{\beta_{21}\cosh(\beta_{21}w)}-\dfrac{30}{t}\dfrac{\lambda}{\alpha}\dfrac{\phi}{t}\dfrac{\mu+\lambda}{\mu}\dfrac{w}{\beta_1^2-\beta_{21}^2}\dfrac{\sinh(\beta_1 x_1)}{\sinh(\beta_1 w)}\end{array}\right)+\frac{\phi}{t}x_1 x_2 \tag{2.6}$$

where

$$\beta_{10}^2=\frac{12\mu}{\alpha t^2},\quad \beta_{11}^2=\frac{12\mu}{k_f t},\quad \beta_1^2=\beta_{10}^2+\beta_{11}^2,\quad \beta_{21}^2=\frac{60\alpha}{\mu t^2}\ \text{and}\ k_f=\frac{E_f t_f}{\left(1-\nu_f^2\right)} \tag{2.7}$$

It is to be noted that in Eqns. (2.1) to (2.7), $\alpha=2\mu+\lambda$ where μ and λ are Lamé's constants; k_f is in-plane stiffness of the reinforcing sheets; E_f and ν_f are, respectively, elasticity modulus and Poisson's ratio of the reinforcing sheets; Δ is the applied vertical displacement and ϕ is the relative rotation of the top face of the layer with respect to its bottom face. Stress distributions can easily be obtained using the displacement-stress relationships of linear elasticity. Due to their lengthy forms, they are not presented here.

3. EFFECT OF REINFORCEMENT FLEXIBILITY ON COMPRESSIVE/BENDING BEHAVIOR OF ELASTOMERIC BEARINGS

For a bonded elastic layer, there are two limiting cases as far as the flexibility of the reinforcing sheets to which the layer is bonded is concerned: the layer behavior approaches its "unbonded (no-reinforcement)" behavior when the "stiffness ratio" of the reinforcing sheets and the layer, i.e., $k^*_f = k_f/(\mu t)$, tends to zero and approaches its "rigidly-reinforced (rigid-reinforcement)" behavior when this ratio tends to infinity. In this section, the effect of reinforcement flexibility on compressive/bending behavior of elastomeric bearings is investigated for bearings with different geometrical and material properties.

The effects of reinforcement flexibility on compression modulus E_c and bending modulus E_b are shown respectively in Figure 2a and Figure 2b for various Poisson's ratios and for two different shape factors; S=5, 30. It is to be noted that shape factor of a strip-shape layer with a thickness t and width $2w$ is simply equal to $S=w/t$. As shown in the figures, reinforcement flexibility affects both moduli in the same way. Bearings' moduli increase with increasing k^*_f until they reach their rigidly-reinforced values. The effect of k^*_f is much more pronounced when S is large and/or ν is close to 0.5. On the other hand, when ν is small, the bearings' stiffnesses become almost insensitive to the changes in k^*_f even when k^*_f takes considerably large values.

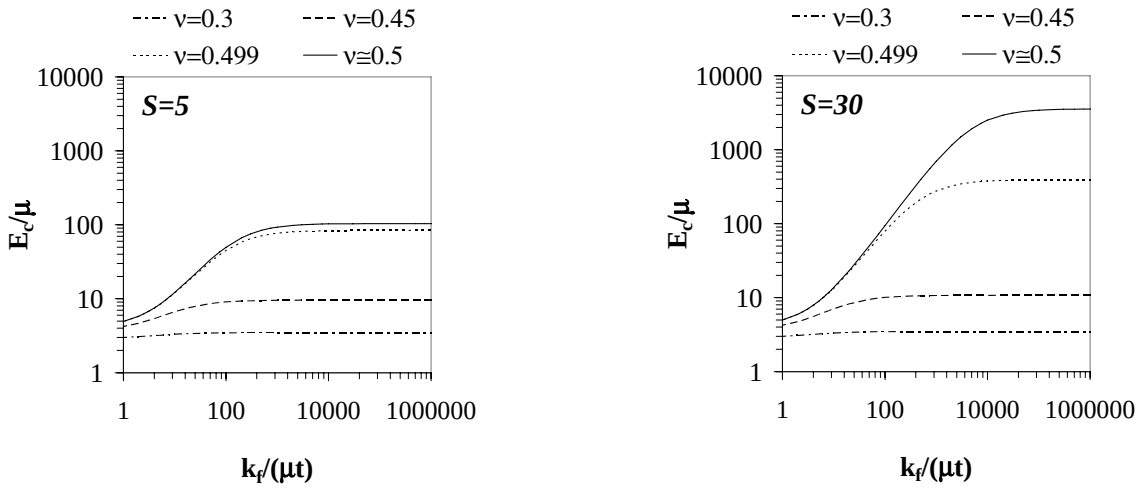

a. effective compression modulus E_c

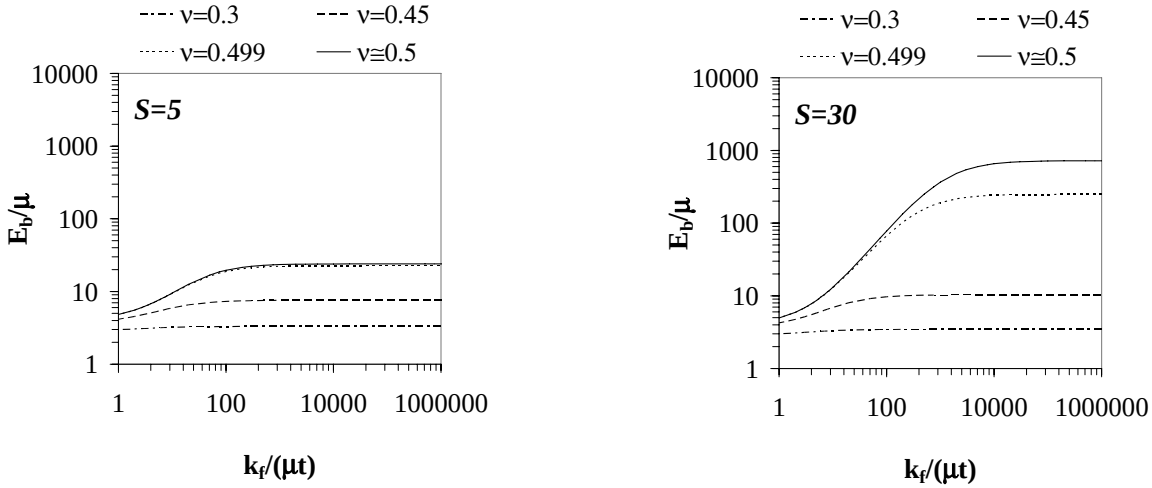

b. effective bending modulus E_b

Figure 2 Effect of reinforcement flexibility on effective moduli of an elastomeric bearing

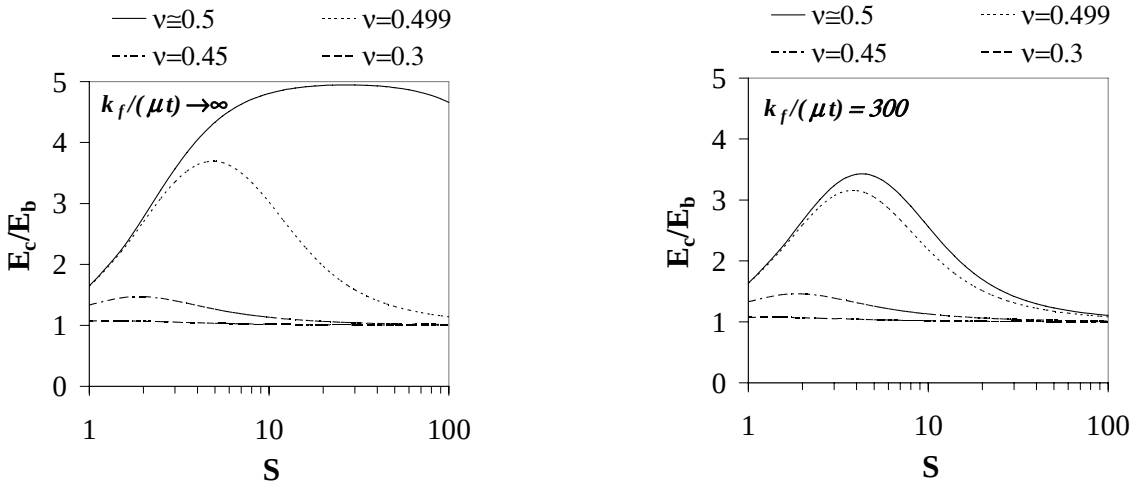

Figure 3 Effect of reinforcement flexibility on E_c/E_b ratio

Due to high resemblance of the graphs in Figure 2b to those in Figure 2a, one may think that the ratio of E_b to E_c is constant. In fact, a factor of five is quoted in the literature (Chalhoub and Kelly, 1991) for E_c/E_b ratio for steel-reinforced strip-shaped bearings. Figure 3 shows the variation of this ratio for bearings of various geometrical and material properties. It is clear that the value quoted in the literature has to be used with caution: E_c/E_b ratio equals to five only when the reinforcements can realistically be assumed to be *rigid*, shape factor of the bearing is considerably large and the layer material is *strictly* incompressible. As shown in Figure 3, reinforcement flexibility can decrease this ratio considerably.

The graphs in Figure 4 show lateral normal stress (τ_{11}) distributions in lateral direction under uniform compression for bearings with two different shape factors; S=1 and S=30, representing, respectively, LSF and HSF bearings. In the graphs, stress values are normalized with respect to the uniform pressure, i.e. $E_c\varepsilon_c$, where $\varepsilon_c=\Delta/t$. Stress distributions for the HSF bearing is plotted for two different k^*_f values; 30000 and 30 (Figure 4a,b). It is worth noting that the value of 30000 for k^*_f, which can be considered as a typical value for a fiber-reinforced rubber bearing, is calculated using the typical values (E_f= 210 GPa, ν_f= 0.3, t_f=0.27 mm, t=3 mm, μ=0.7 MPa) quoted in literature (see, e.g., Kelly, 2002). Although similar graphs (with both k^*_f=30000 and k^*_f=30) have also been plotted for the LSF bearing, it has been seen that there is almost no difference between these two graphs, indicating that the behavior of the LSF bearing is insensitive to the reinforcement flexibility even when k^*_f is as low as 30. For this reason, only one graph is included in Figure 4 for the bearing with S=1. At this point, it is important to note that this surely does *not* mean that LSF bearings are *not* influenced from reinforcement flexibility. Since they reach their rigid-reinforcement behavior at much smaller values of k^*_f (see Figure 2), k^*_f has to be considerably low for this type of bearings to start to "sense" the reinforcement flexibility.

As shown in Figure 4a,b, the effect of reinforcement flexibility on lateral normal stress distributions in the HSF bearing is significant when the layer material is nearly incompressible. As k^*_f decreases, maximum lateral normal stress which occurs at point (x_1=0, x_2=0) decreases significantly and parabolic stress distributions become much more uniform. Analyses show that k^*_f has the same effect on axial stress distributions in lateral direction. In fact, it can be seen that k^*_f has exactly the same effect on stress distributions in an elastomeric bearing as ν has. From Figure 4a,b, it can also be seen that as reinforcement flexibility increases, the dramatic difference between the behavior of bearings with strictly incompressible and nearly incompressible materials decreases. The main reason for such a change in the behavior is the fact that a bearing with a smaller k^*_f attains its "incompressible" modulus at a smaller value of ν (Pinarbasi and Mengi, 2008).

Figure 5 presents similar graphs plotted for the pure bending case. In these graphs, stress values are normalized by $SE_b\phi$, which corresponds to the maximum bending stress developing in the corresponding unbonded layer as predicted by the simple beam theory. It is to be noted that the shape factor of the LSF bearing is selected in this case as 2.5. At this point, it is noteworthy that, the S values for the LSF bearings are selected to be equal to the most critical shape factor as far as the normalized shear stress is concerned. While this critical value is 1.0 for the uniform compression case, it is 2.5 for the pure bending case in strip-shaped bearings (see Figure 8). Figure 5 clearly shows that the same conclusions derived for the compression case are valid also for the bending case: the effect of k^*_f on stress distributions is exactly the same as that of ν. The shapes of the stress distributions under pure bending are surely different than those under uniform compression: the polynomial-like distribution of normal stresses tends to a linear distribution with a shift on the location of peak stress towards the edge as k^*_f or ν decreases.

From the graphs in Figure 6, which plot normal (τ_{11} and τ_{22}) and shear (τ_{12}) stress distributions in axial direction in a uniformly compressed bearing with S=1 and k^*_f=30, one can see that, the "pressure assumption" is *not* valid for LSF layers bonded to flexible reinforcements: normal stresses are neither constant nor equal to each other through the layer thickness. In addition, shear stress distributions may also become highly nonlinear in vertical direction. Our studies show that a similar conclusion is valid for HSF layers if the reinforcement stiffness and/or Poisson's ratio is low. While normal stresses in an HSF layer are constant through the layer thickness even when k^*_f =30 or ν=0.3, axial stress distributions start to deviate from lateral stress distributions as k^*_f or ν decreases. This can be seen from normal stress distributions plotted in Figure 7 for a purely bended bearing with S=30, which are identical in shape to the compression case.

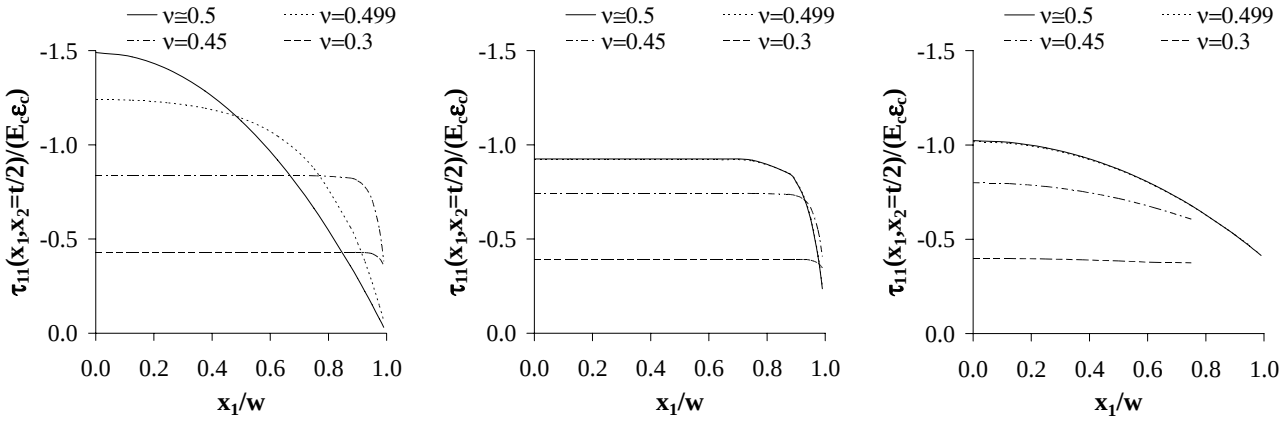

a. S=30, $k_f/\mu t$ = 30000 b. S=30, $k_f/\mu t$ = 30 c. S=1, $k_f/\mu t$ = 30

Figure 4 Lateral normal stress distributions in lateral direction under uniform compression

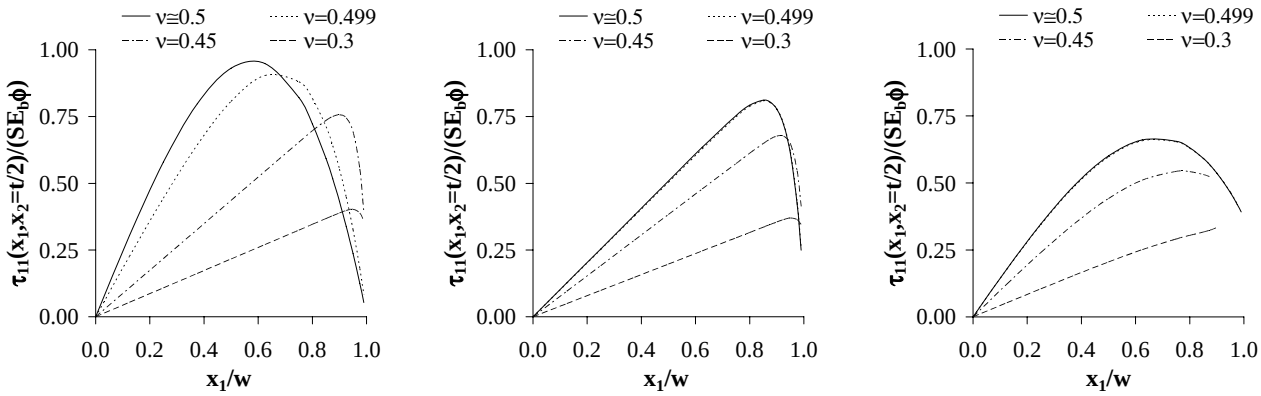

a. S=30, $k_f/\mu t$ = 30000 b. S=30, $k_f/\mu t$ = 30 c. S=2.5, $k_f/\mu t$ = 30

Figure 5 Lateral normal stress distributions in lateral direction under pure bending

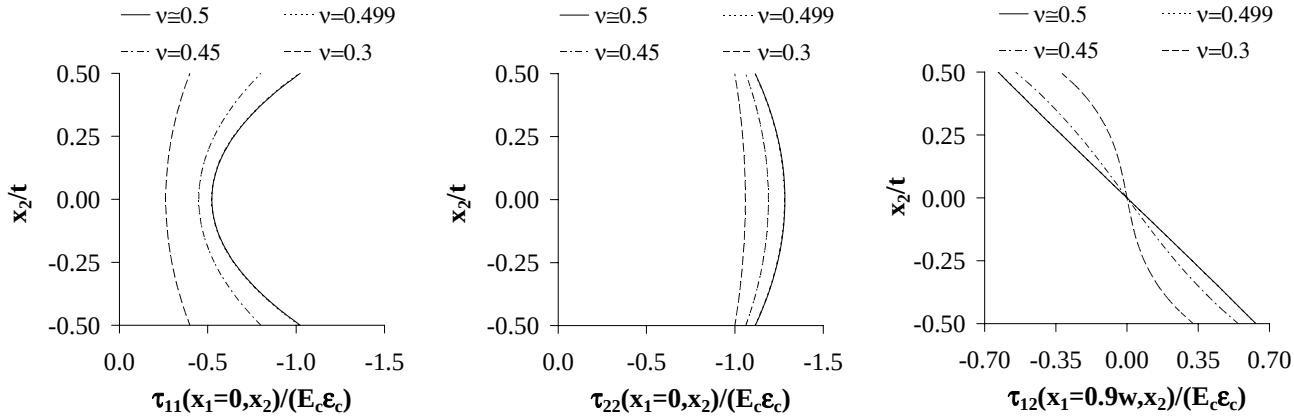

Figure 6 Normal and shear stress distributions in axial direction under uniform compression for S=1 and when $k_f/\mu t$ =30

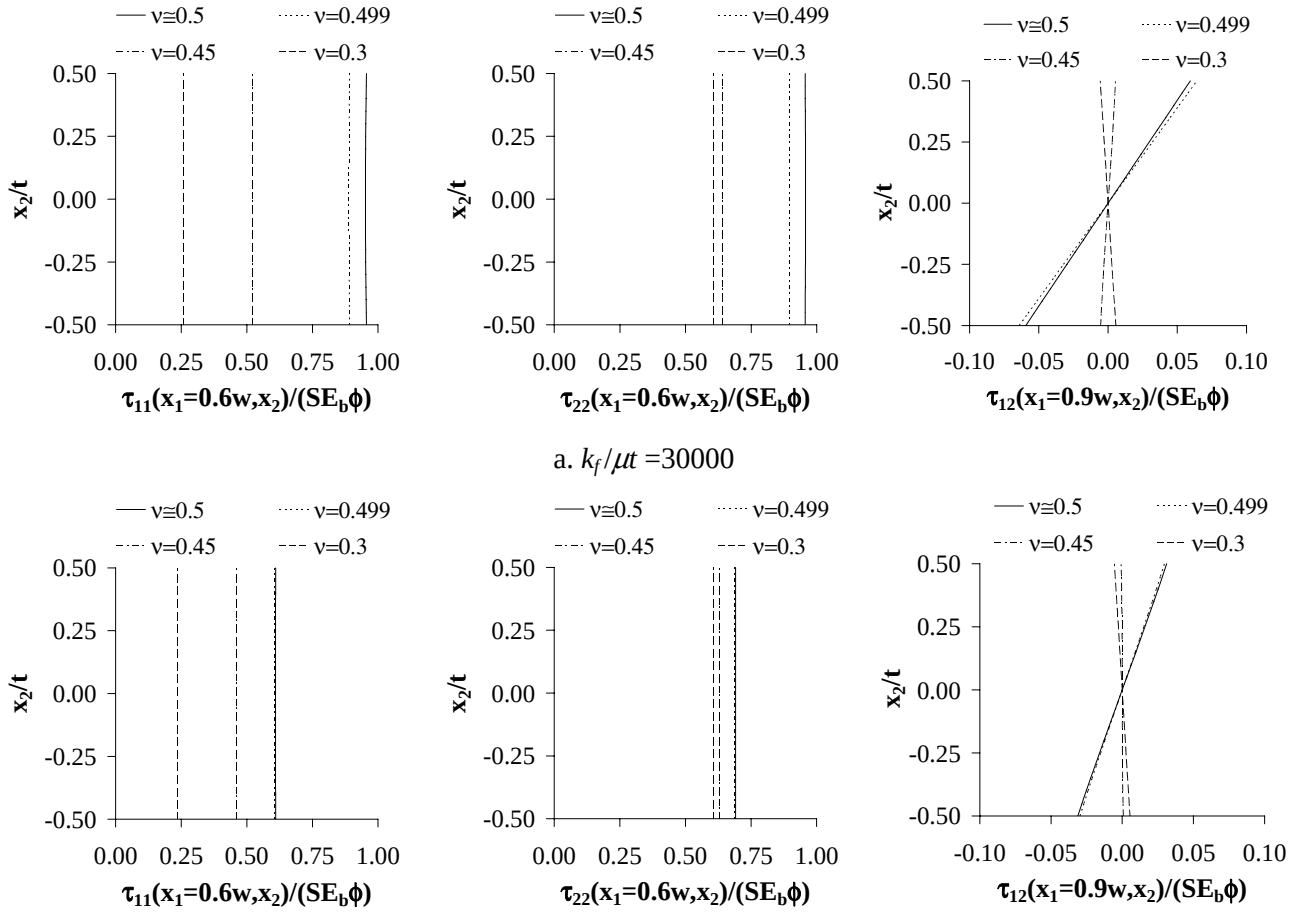

a. $k_f/\mu t$ =30000

b. $k_f/\mu t$ =30

Figure 7 Effect of reinforcement flexibility on normal and shear stress distributions in axial direction under pure bending for S=30

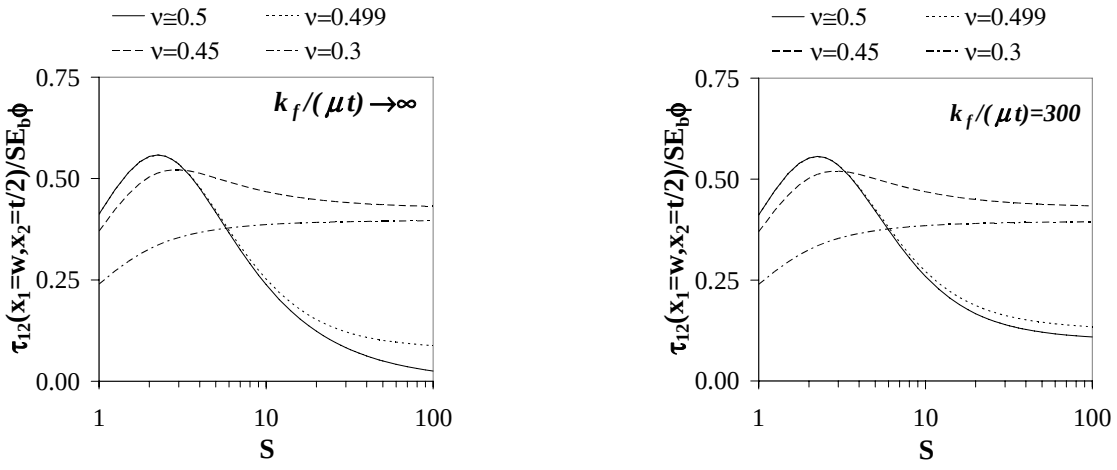

Figure 8 Maximum normalized shear stress in a reinforced elastomeric bearing with different geometrical and material properties

One of the most important design parameters for elastomeric bearings is the maximum shear strain that develops in the elastomer layers. In most engineering practices, multi-layered elastomeric bearings are designed for combined action of compression and/or bending and shear. It is now very well-known that due to the restraint of elastomer bulging by the reinforcing plates at the bonded faces, considerable amount of additional shear strain may develop in a multi-layered elastomeric bearing subjected to compression and/or bending. Thus, in order to compute the maximum shear strain in an elastomeric bearing, the shear strain developed due to compression and/or bending has to be added to the shear strain created directly by the applied shear forces. Our studies show that, under uniform compression or pure bending, maximum shear stress, so maximum shear strain, occurs at the edges of the bonded faces, i.e., at points ($x_1=\pm w$, $x_2=\pm t/2$), in an elastomer layer. Figure 8 shows the variation of maximum shear stress in a purely bended elastomeric bearing with its shape factor for two different stiffness ratios. Parallel with the earlier conclusions, reinforcement flexibility is observed to be most effective when S is sufficiently large and ν is sufficiently close to 0.5. From the graphs, it should *not* mistakenly be understood that the shear stress developing in an HSF bearing is usually much smaller than that in an LSF bearing. While interpreting on these graphs, it should be kept in mind that the graphs plot the "normalized" stress values and SE_b of an HSF bearing can be much larger than that of an LSF bearing.

4. CONCLUSIONS

Bearings composed of several elastomer layers bonded to reinforcing sheets are widely used in many engineering applications. While, in most of the earlier applications, steel shim plates have been used as reinforcing agents in multi-layered elastomeric bearings, recent studies propose the use of flexible fiber reinforcement. In this way, it is believed to be possible to produce both light-weight and cost-effective isolators to be used in low-cost housing.

Although the "rigid" reinforcement assumption is a fairly reasonable assumption in the analysis of a steel-reinforced bearing, it is necessary to include the effect of reinforcement flexibility while studying the compressive or bending behavior of a fiber-reinforced bearing. This study investigates the effect of reinforcement flexibility on behavior of elastomeric bearings under uniform compression and pure bending.

Analyses conducted on bearings with different geometrical and material properties show that the compressive/bending behavior of a fiber-reinforced bearing can be considerably different than that of its steel-reinforced counterpart. In general, it can be said that reinforcement extensibility has the same effect on bearing behavior as material compressibility has. For this reason, the effect of reinforcement flexibility highly depends on the geometrical and material properties of the bearing. It can also be concluded that reinforcement flexibility is most effective when the "shape" factor of the bearing is large and Poisson's ratio of the layer material is close to 0.5.

REFERENCES

Chalhoub, M.S., Kelly, J.M. (1991). Analysis of infinite-strip-shaped based isolator with elastomer bulk compression. *Journal of Engineering Mechanics* **117**, 1791-1805.

Kelly, J.M. (1997). Earthquake resistant design with rubber. Springer-Verlag, London.

Kelly, J.M. (2002). Seismic isolation systems for developing countries. *Earthquake Spectra* **18:3**, 385-406.

Mengi, Y. (1980). A new approach for developing dynamic theories for structural elements Part 1: Application to thermoelastic plates. *International Journal of Solids and Structures* **16**, 1155-1168.

Moon, B.-Y., Kong, G.-J., Kong, B.-S., Kelly, J.M. (2002). Design and manufacturing of fiber reinforced elastomeric isolator for seismic isolation. *Journal of Materials Processing Technology* **130-131**, 145-150.

Pinarbasi, S., Mengi, Y. (2008). Elastic layers bonded to flexible reinforcements. *International Journal of Solids and Structures* **45**, 794-820.

Tsai, H.-C. (2004). Compression stiffness of infinite-strip bearings of laminated elastic material interleaving with flexible reinforcements. *International Journal of Solids and Structures* **41:24-25**, 6647-6660.